Received: 07 April 2020 | Revised: 26 August 2020 | Accepted: 28 August 2020
DOI: 10.22034/ecc.2020.113346
Eurasian Chemical Communications
SAMI

FULL PAPER

Synthesis, characterization, density functional theory (DFT) calculation and antibacterial activities of five-coordinate complexes of some first-row transition metals containing a benzoyl thiourea derivative

Javad Farzanfar[a,b] |Elahe Abdolahe[b] |Amir Eskandari[b] |Ali Reza Rezvani[b,*] |Hojat Samareh Delarami[c]

[a]*Pharmaceutical Sciences Research Center, Shiraz University of Medical Sciences, Shiraz, Iran*

[b]*Department of Chemistry, University of Sistan and Baluchestan, Zahedan, Iran*

[c]*Department of Chemistry, University of Zabol, Zabol, Iran*

***Corresponding Author:**
Ali Reza Rezvani
Email: Ali@hamoon.usb.ac.ir
Tel.: +98 54 31136249

Using elemental analysis, Fourier transform infrared (FTIR) and UV-visible spectroscopies, as well as conductivity measurements, synthesis of 5 first-row transition metal complexes, including $[M(L')(H_2O)_2]$ (M=Mn (C1), Fe (C2), Co (C3), Ni (C4), Cu (C5)) relevant to a benzoyl thiourea ligand, which was derived by condensing 2-chlorobenzoyl-isothiocyanate with 2,6-diaminopyridine, to produce 1,1'-(pyridine-2,6-diyl)bis(3-(2-chlorobenzoyl) thiourea) (L) was conducted. The structures proposed for the five complexes were confirmed through the application of conformational analysis and geometry optimization. These compounds were studied in vitro in terms of antibacterial properties against the standard gram-positive and gram-negative bacterial strains, and their superior antibacterial activities compared to those of the new thiourea derivative were proven through the experiments.

KEYWORDS

Density functional theory (DFT); antibacterial activity; benzoyl thiourea; complex; 2-chlorobenzoyl-isothiocyanate.

Introduction

In recent years, many studies have focused on developing efficient antimicrobial agents to inhibit the growths of various drug-resistant strains [1,2]. According to the pharmacological investigations of the carbonyl- and thiocarbonyl-containing compounds, including as urea and thiourea and their related analogs, thiourea derivatives and transition metal complexes have been proposed to have a wide variety of biological functions, such as antibacterial [1-9], antifungal [6-11], anti-diabetic [12], anti-tubercular [13], anti-human immunodeficiency virus (anti-HIV) [14], anti-hepatitis C virus (anti-HCV) [15,16], antitumor [17,18], anti-thyroid, anthelmintic, rodenticidal, insecticidal, and herbicidal properties, as well as activities of plant-growth regulators [19-21]. In many studies, the application of a range of metal ions for coordinating thiourea derivatives as potential donor ligands has led to the enhanced biological activities of these compounds. Therefore, complexation revealed a novel approach to dose reduction [22]. Having incredible natural properties, some first-row transition metals are considered as physiologically essential elements in trace amounts. At the same time, their combination with thiourea derivatives can result in the

generation of improved antimicrobial agents [23].

The coordination of thiourea-based ligands together with first-row transition metal ions results in superior lipophilicity of transition metal atom and therefore, its premiere lipid bilayer permeance via the decrement of the polarity of the transition metal cation with partial sharing of positive charge of transition metal cation together with donor atoms of thiourea-derived ligands and delocalization of electron upon the chelating [23].

For this reason, we aimed at synthesizing and characterizing the antibacterial activities of new complexes produced from 5 first-row transition metals associated with 1, 1'-(pyridine-2, 6-diyl)bis(3-(2-chlorobenzoyl)thiourea) (L) as a thiourea derivative. For validating the proposed structures, geometry optimization and conformational analysis were applied as a supplementary tool for all the complexes due to inaccessibility to suitable crystals from pure solid thiourea compounds for X-ray measurements. The in vitro screening of all the compounds was done to detect their antibacterial activities against Staphylococcus aureus and Enterococcus faecalis and Escherichia coli and Pseudomonas aeruginosa as two standard gram-positive and two standard gram-negative bacterial strains, respectively.

Experimental procedure

Materials and instrumentation

Upon receiving all the starting reagents andsolvents from Sigma-Aldrich and Merck, they were utilized to perform the elemental analyses using a Leco, CHNS-932 elemental analyzer. A FT-IR JASCO 680-PLUS spectrometer was employed to record the infrared spectra as KBr pellets within the spectral range of 4000–400 cm^{-1}. Using the quartz cells with a 10-mm pass length, recording of the electronic spectra (UV-visible (UV-Vis)) on a UV-JASCO-570 spectrometer was conducted at room temperature. A Ciba Corning model check-mate 90 conductivity meter was employed to measure the molar conductivity at room temperature by using a sample N, N-dimethylformamide (DMF) solution (10^{-3} M).

Synthesis of transition metal complexes containing a benzoyl thiourea derivative

1,1'-(Pyridine-2, 6-diyl)bis(3-(2-chlorobenzoyl)thiourea) (L) has been previously synthesized and characterized [23]. Similar to what has been described in the literature, ligand L was synthesized [24,25] *via* a reaction between two mmol of 2-chlorobenzoyl chloride and two mmol of NH_4SCN in acetone to make it condense with one mmol of 2,6-diaminopyridine. Based on the procedure described in the literature, preparation of the five first-row transition metal complexes was followed [23,26] through another reaction between 10 mL of aqueous solutions of the transition metal chlorides of Mn^{II} (C1), Fe^{II} (C2), Co^{II} (C3), Ni^{II} (C4), and Cu^{II} (C5) (1 mmol) separately and 10 mL of an ethanol solution of the ligand (1 mmol) using triethyl amine. Isolation of the complexes as solids was achieved after refluxing the reaction mixtures for 48 h. Regarding the solubility of all the solid products in acetone, dichloromethane, dimethyl sulfoxide (DMSO), and N, N-dimethylformamide (DMF), their re-crystallizations from an ethanol-dichloromethane mixture (1:2) was readily performed.

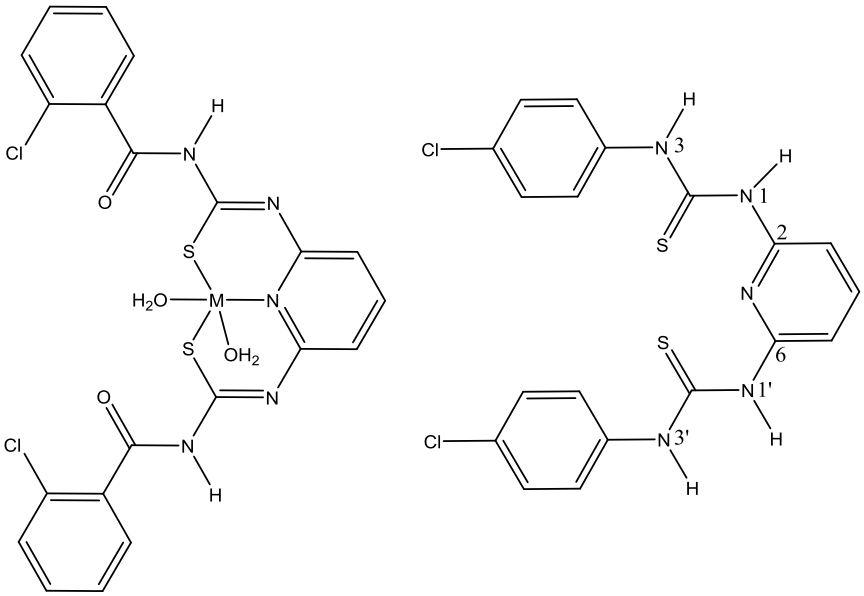

SCHEME 1 Schematic presentation of the complexes and ligand

C1: Anal. Calc. For $C_{21}H_{17}Cl_2MnN_5O_4S_2$ (%; FW: 593.36 g.mol^{-1}): C, 42.51; H, 2.89; N, 11.80; S, 10.81; Found: C, 42.49; H, 2.87; N, 11.85; S, 10.83. FT-IR (KBr, cm^{-1}): 3427.5, 3332.7, 3221.7, 3192.9, 3111.9, 3045.1, 1675.9, 1637.1, 1592.3, 1577.4, 1532.8, 1438.1, 1303.1, 1222.8, 1207.5, 1161.7, 1096.8, 1045.3, 999.4, 947.8, 840.9, 798.1, 771.4, 745.2, 709.7, 690.3, 648.8, 613.8, 571.1, 479.9. UV-Vis (DMSO, nm): 229, 322. Λ_M (DMF, ohm^{-1} cm^2 mol^{-1}) = 48.

C2: Anal. Calc. For $C_{21}H_{17}Cl_2FeN_5O_4S_2$ (%; FW: 594.27 g.mol^{-1}): C, 42.44; H, 2.88; N, 11.78; S, 10.79; Found: C, 42.41; H, 2.84; N, 11.81; S, 10.82. FT-IR (KBr, cm^{-1}): 3426.2, 3392.6, 3220.7, 3180.4, 3111.6, 3046.4, 1676.3, 1591.9, 1577.5, 1555.9, 1534.4, 1477.2, 1439.9, 1402.5, 1301.7, 1220.9, 1209.8, 1161.5, 1044.5, 1021.7, 946.2, 882.9, 844.3, 796.7, 771.6, 708.9, 692.7, 660.6, 616.1, 570.4, 496.7, 468.1, 438.5. UV-Vis (DMSO, nm): 231, 323, 475, 581, 915. Λ_M (DMF, ohm^{-1} cm^2 mol^{-1}) = 42.

C3: Anal. Calc. For $C_{21}H_{17}Cl_2CoN_5O_4S_2$ (%; FW: 597.36 g.mol^{-1}): C, 42.22; H, 2.87; N, 11.72; S, 10.74; Found: C, 42.18; H, 2.84; N, 11.74; S, 10.78. FT-IR (KBr, cm-1): 3414.6, 3384.1, 3219.3, 3175.5, 3111.9, 3047.1, 1671.4, 1589.2, 1550.4, 1536.2, 1439.5, 1305.8, 1214.9, 1158.8, 1117.9, 1050.6, 841.2, 795.4, 709.2, 688.6, 611.5, 474.6. UV-Vis (DMSO, nm): 228, 321, 458, 474, 861. Λ_M (DMF, ohm^{-1} cm^2 mol^{-1}) = 50.

C4: Anal. Calc. For $C_{21}H_{17}Cl_2N_5NiO_4S_2$ (%; FW: 597.12 g.mol^{-1}): C, 42.24; H, 2.87; N, 11.73; S, 10.74; Found: C, 42.19; H, 2.82; N, 11.78; S, 10.79. FT-IR (KBr, cm^{-1}): 3421.8, 3313.4, 3226.1, 3039.9, 1675.9, 1578.9, 1539.1, 1439.6, 1304.7, 1221.6, 1209.2, 1208.7, 1160.3, 1126.4, 1112.6, 1043.9, 845.7, 797.6, 771.8, 706.6, 689.6, 614.2, 438.3. UV-Vis (DMSO, nm): 231, 319, 568, 791, 882. Λ_M (DMF, ohm^{-1} cm^2 mol^{-1}) = 45.

C5: Anal. Calc. For $C_{21}H_{17}Cl_2CuN_5O_4S_2$ (%; FW: 601.97 g.mol^{-1}): C, 41.90; H, 2.85; N, 11.63; S, 10.65; Found: C, 41.85; H, 2.82; N, 11.67; S, 10.69. FT-IR (KBr, cm^{-1}): 3435.2, 3356.8, 3221.2, 3111.4, 3048.4, 1676.6, 1591.7, 1577.2, 1533.7, 1448.7, 1439.6, 1401.1, 1303.6, 1260.1, 1220.4, 1161.2, 1097.4, 1044.3, 1021.9, 946.7, 844.6, 793.3, 771.4, 705.3, 685.3, 612.9, 570.2, 496.3, 438.5. UV-Vis (DMSO, nm): 229, 321, 512, 675, 931. Λ_M (DMF, ohm^{-1} cm^2 mol^{-1}) = 51.

Theoretical computations

Geometric optimization and conformational analysis were performed in the gas phase to

accurately understand the molecular structures of the five first-row transition metal complexes, which contained a benzoyl thiourea derivative through the application of Gaussian 09 suite of programs and Beck's 3-parameter hybrid method at the B3LYP level with the 6-31G (d, p) basis set. To ensure the local minimum of the structures, vibrational frequencies were also analyzed at the same level. The Natural Bond Orbital (NBO) 3.1 program was utilized on the wave functions to obtain the NBO analysis at the same level of the theory [27-30].

Antibacterial test

The in vitro antibacterial assay was carried out against two gram-negative and two gram-positive standard strains of bacteria, i.e., Escherichia coli: E. coli ATCC 25922 and Pseudomonas aeruginosa: P. aeruginosa ATCC 27853 and Staphylococcus aureus: S. aureus ATCC 25923 and Enterococcus faecalis: E. faecalis ATCC 11700, respectively.

Determination of minimum inhibitory concentration (MIC)

Minimum inhibitory concentration (MIC) is defined as the lowest concentration of the compounds that lead to the prevention of visible bacterial growth after incubation at 36 °C for 18 h. The MICs of all the synthesized complexes against the above-mentioned standard bacterial strains were studied through a broth macro dilution assay in a sterile test tube [31] and by using the Muller Hinton Broth (MLB) medium. To prepare the stock solutions, DMSO was applied as a solvent and a negative control since it had no effects on the microorganisms. Then, further dilutions with distilled water were conducted. The assayed compounds had the concentrations of 1024, 896, 768, 640, 512, 256, 128, 64, 32, 16, 8, 4, 2, and 1 µg/mL. A fresh bacterial culture was prepared in a nutrient broth medium within 24 h. As a standard of turbidity, McFarland Standard 0.5 solution was employed to compare the turbidities of the bacterial cultures. Assessment of the incubation results of all the inoculated tubes at 36 °C was done for the bacteria after 18 h.

Inhibition zone determination

Using a disk diffusion method, the in vitro inhibition zones of the synthesized compounds against all the standard bacterial strains were determined. Some sterilized paper disks with 6-mm diameter were immersed in the DMSO solution of the tested compounds at a concentration of equal to most MICs obtained for 5 min. Then, they were attached to the surfaces of Muller-Hinton agar (MHA) plates inoculated with the adequate inoculum loop (0.01 cm^3) of the bacteria (10^6 CFUs cm^{-3}). Besides using DMSO as a negative control, Amikacin (AMK-30 µg) and Gentamycin (GEN-10 µg) were applied as positive controls for the gram-positive and gram-negative antibacterial activities, respectively. The diameter of each inhibition zone resulted from the incubation of all the plates was measured at 36 °C for 24 h without any bacterial growths.

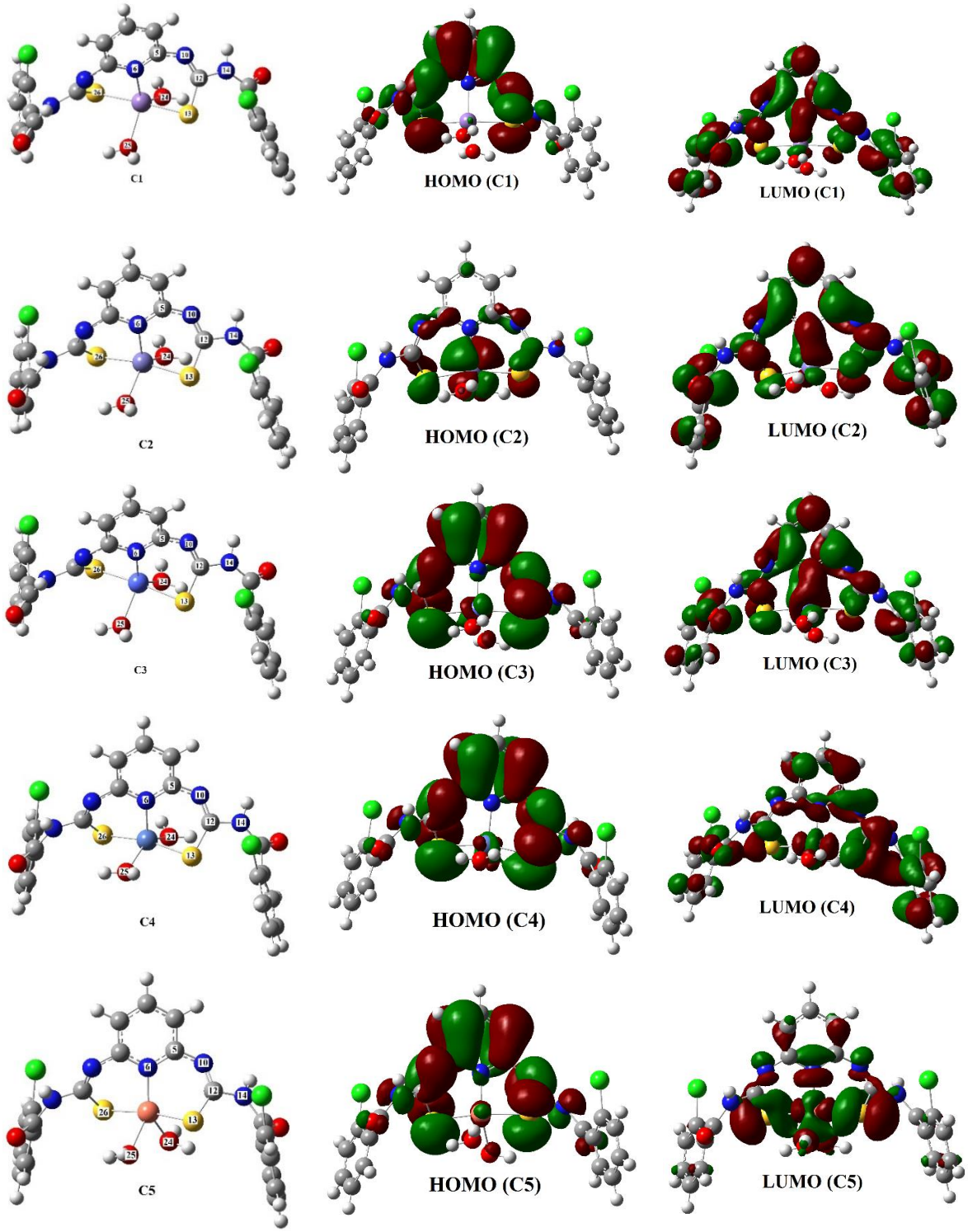

FIGURE 1 The minimum energy structures and HOMO and LUMO molecular orbitals of the complexes

Results and discussion

Infrared spectroscopy

Using infrared spectroscopy, the solid-state properties of the five new complexes were studied. All the expected frequency regions of ν(N—H), ν(C═S), ν(C═O), and ν(C—N) were exhibited by the infrared spectra of the mentioned samples. Thiourea ligand (L) behavior as a bi-negative tridentate chelating

agent was observed to provide coordination between pyridyl group nitrogen, as well as the two CS groups in the form of thiol and each of the five transition metal ions in the suggested structures of the complexes (Figure 1). There was a pentacoordinate environment around each of the mentioned transition metal atoms. A change into lower frequencies and a weakening due to the complexation occurred to two characteristic IR bands (at about 1305 and 1220 cm^{-1}) and another characteristic IR ν(C═S) band (at around 840 cm^{-1}), which were associated with the stretching vibrations of thionyl (C═S) groups of a free thiourea ligand in the regions of 1325-1351 and 1239-1260 cm^{-1} and the area of 824-844 cm^{-1} within the IR spectra of the mentioned complexes, respectively. The structures proposed for these complexes were observed to be acceptable as the C=S groups were seen to participate in the mentioned coordination [32]. ν(C—N) stretching vibrations resulted in the multiple high and medium intensities of absorption bands within a range of 1000–1200 cm^{-1}. Also, the stretching vibration of the carbonyl (C═O) group led to a sharp band of absorption at about 1670 cm^{-1}. ν(Ph—H) stretching mode was the result of the absorption band at around 3040 cm^{-1}.

Moreover, the pyridine ring was found to have a ν(C=C) + ν(C=N) vibration frequency at about 1515-1600 cm^{-1}. Pyridine group was observed to be involved in the ring wagging vibrations of 680-692 and 792-799 cm^{-1}. The in-plane pyridine ring deformation was ascribed to the absorption band at nearly 610 cm^{-1} [23]. Besides, ν(C—Cl) stretching vibration of the phenyl ring in thiourea ligand L had an absorption band of 710 cm^{-1} [25, 26]. ν(H_2O) stretching vibrations of the coordinated water molecules were the reason for the broad characteristic IR absorption band at about 3425 cm^{-1} within the IR spectra of the present complexes. This wide broadness represented an intensive H-bonding [23].

TABLE 1 The selected angles (°) of DFT of thiourea complexes

	C1	C2	C3	C4	C5
Angle (°)					
N6-C5-N10	123.5352	124.3229	124.1443	124.6243	123.7132
C5-N10-C12	130.3535	130.8692	129.2791	129.7077	127.0319
N10-C12-S13	130.4587	130.7525	129.7279	130.0429	128.6787
N10-C12-N14	111.6626	111.6056	111.6652	111.5373	112.3240
C12-S13-M	92.19617	93.91997	93.53780	94.37164	92.83601
S13-M-N6	92.18439	95.50041	92.91052	96.95722	93.89482
S13-M-O24	89.53702	89.33545	83.30934	89.45233	86.46620
S13-M-O25	89.13019	85.65343	85.59863	85.71571	87.92282
S13-M-S26	175.6358	168.9685	171.3979	166.1316	172.2706
S26-M-N6	92.16602	95.52998	95.57386	96.91064	93.83075
S26-M-O24	88.41199	85.65212	90.28538	85.65429	87.78014
S26-M-O25	88.06234	89.71657	91.51759	89.69620	86.75766
N6-M-O24	122.5879	116.2177	128.4691	110.1753	136.3231
N6-M-O25	125.4909	115.6605	118.957	109.8712	135.3092
O24-M-O25	111.9099	128.1214	111.9729	139.9535	88.36773

Electronic absorption spectroscopy

After preparing DMSO solutions of the five new complexes containing the thiourea ligand (L), their electronic absorption spectra were recorded within the range of 200-1000 nm. Several absorption bands were displayed in the UV and visible regions as the electronic excitation of the samples was studied in the DMSO solution. Within the thiourea moieties of the complexes, the intra-ligand π→π* and n→π* transitions of the charge transfer from phenyl and pyridine rings were associated with two intense absorption bands at nearly

230 and 320 nm for the present complexes of C1, C2, C3, C4, and C5 in the UV region. According to the literature [33], several characteristic transition bands of ligand field d–d are displayed by the 5-coordinate metal complexes of high-spin transitions with square pyramidal geometries at low intensities within the visible region. The high-spin Mn(II) center of the 5-coordinate square pyramidal geometry could be attributed to the presence of no apparent transition bands of ligand field d–d within the visible region of the electronic spectrum of Mn(II) complex (C1). The three weak absorption bands of transitions $^5E \rightarrow {}^5B_2$, $^5E \rightarrow {}^5A_1$, and $^5E \rightarrow {}^5B_1$ at 915, 581, and 475 nm were found for the electronic spectrum of Fe(II) complex (C2) within the visible region, respectively, which were indicative of the presence of a square pyramidal geometry. Also, the three weak absorption bands of $^4A_2 + {}^4E \rightarrow {}^4B_1$, $^4A_2 + {}^4E \rightarrow {}^4E$ (P), and $^4A_2 + {}^4E \rightarrow {}^4A_2$ (P) transitions at 861, 474, and 458 nm were observed for the electronic spectrum of Co(II) complex (C3) within the visible region, respectively, which represented a square pyramidal geometry as well. This square pyramidal geometry was further discovered for the electronic spectrum of Ni(II) complex (C4) within the visible region as exhibited by the three weak absorption bands of transitions $^3B_1 \rightarrow {}^3A_2$, $^3B_1 \rightarrow {}^3B_2$, and $^3B_1 \rightarrow {}^3E$ at 882, 791, and 568 nm, respectively. Finally, the electronic spectrum of Cu(II) complex (C5) within the visible region demonstrated the three weak absorption bands of $^2A_1 \rightarrow {}^2B_1$, $^2B_2 \rightarrow {}^2B_1$, and $^2E \rightarrow {}^2B_1$ transitions at 931, 675, and 512 nm, respectively, also suggesting a square pyramidal geometry

TABLE 2 The selected bond lengths [Å] of DFT of thiourea complexes

	C1	C2	C3	C4	C5
Bond Length (Å)					
N6-C5	1.3655	1.37101	1.36972	1.36863	1.36609
C5-N10	1.37888	1.37502	1.37505	1.37651	1.37681
N10-C12	1.29531	1.29582	1.29681	1.29832	1.2963
C12-S13	1.76275	1.7595	1.75457	1.75173	1.75632
C12-N14	1.40773	1.40699	1.40606	1.40562	1.4018
M-S13	2.46481	2.39204	2.43800	2.34329	2.31872
M-S26	2.45604	2.39115	2.35181	2.34423	2.31894
M-N6	2.13873	2.0622	2.02463	1.98066	1.95689
M-O24	2.22498	2.19925	2.13159	2.10741	2.19364
M-O25	2.22435	2.20104	2.13734	2.10723	2.19672

Measurement of molar conductivity

A range of 42-51 ohm^{-1} cm^2 mol^{-1} was measured for the molar conductance in the DMF solution (10^{-3} M). The formulae of the complexes were well corroborated to be within an expected range, as mentioned for non-electrolytes in the related literature and thus provided the desired structural information [34].

TABLE 3 Some theoretically computed HOMO, LUMO energies, dipole moments, and atom charges of thiourea complexes

Charge	C1	C2	C3	C4	C5
N6	-0.63486	-0.63495	-0.62052	-0.60307	-0.59631
N10	-0.57463	-0.57213	-0.57358	-0.58149	-0.56848
N14	-0.65701	-0.65701	-0.65621	-0.65706	-0.65571
C12	0.30687	0.30353	0.30487	0.29583	0.29923
S13	-0.37133	-0.34182	-0.33096	-0.28547	-0.26004
S26	-0.37625	-0.33966	-0.29715	-0.28450	-0.25911
O24	-0.96347	-0.95707	-0.94992	-0.93900	-0.94259
O25	-0.96411	-0.95685	-0.94663	-0.93880	-0.94263
E_{HOMO} (a.u.)	-0.1899	-0.20012	-0.20258	-0.20711	-0.20934
E_{LUMO} (a.u.)	-0.06111	-0.06276	-0.06323	-0.06442	-0.06595
ΔE_{L-H}	0.12879	0.13736	0.13935	0.14269	0.14339
μ (debye)	3.5499	2.6719	3.0913	1.6432	2.5450

Computational investigation

The molecular structures of the five new complexes containing thiourea ligand (L) were optimized at the DFT level of the theory. Tables 1 and 2 represent the major geometrical parameters of the target compounds. A configuration ranging from Regular Trigonal Bi-Pyramidal (RTBP) to Regular Square-Based Pyramidal (RSBP) coordinations were found for the transition metal complexes of 5-coordinate atoms around the metal ions. The compounds were found to have an RSBP configuration, and the coordination with the transition metal ions was inferred to have occurred through pyridyl group nitrogen and two CS groups in the form of thiol since the angles of N6-M-O24, N6-M-O25, O24-M-O25, N6-M-S13, N6-M-S26, S13-M-O24, S13-M-O25, S13-M-S26, S26-M-O24, and S26-M-O25 were within the ranges of 110.17° in C4 to 136.32° in C5, 109.87° in C4 to 135.31° in C5, 88.37° in C5 to 139.95° in C4, 92.18° in C1 to 96.96° in C4, 92.17° in C1 to 96.91° in C4, 83.31° in C3 to 89.54° in C1, 85.60° in C3 to 89.13° in C1, 166.13° in C4 to 175.63° in C1, 85.65° in C2 to 90.28° in C3, and 86.76° in C5 to 91.52° in C3, respectively. A shorter bond length of N10-C12 and longer bond lengths of C12-S13 and N6-C5 than that of thiourea ligand (L) were observed in the complexes, as shown in Table 2 [23]. These results confirmed the suggested coordination with the transition metal ions through pyridyl group nitrogen and the two CS groups in thiol form. Figure 1 presents the frontier highest occupied molecular orbital (HOMO) and lowest unoccupied molecular orbital (LUMO) of the five complexes. Table 3 illustrates some remarkable electronic characteristics, including calculated natural atom charges, dipole moments, and HOMO and LUMO energies for all the compounds. As can be seen, higher negative charge densities in the HOMO molecular orbitals occur around sulfur atoms of thiourea ligand (L), which can enhance the probability of nucleophilic attack from those atoms to metal ions. The interaction between electron donors and acceptors are facilitated by higher HOMO and lower LUMO energies. Based on the results obtained from the previous antibacterial studies [35], the antibacterial activities of these compounds significantly depend on the amount of difference between LUMO and HOMO energies (ΔE_{L-H}) and LUMO energy (E_{LUMO}) level.

TABLE 4 The values of minimal inhibitory concentrations (MIC, µg/mL) and zones of inhibitions (ZI, diameter/mm) of all compounds against the studied bacterial strains

Samples	E. coli		P. aeruginosa		S. aureus		E. faecalis	
	MIC	ZI	MIC	ZI	MIC	ZI	MIC	ZI
C1	512	11.80	256	16.48	128	9.28	512	9.84
C2	512	9.12	128	19.12	128	9.02	512	12.42
C3	640	9.68	256	17.30	128	8.72	512	12.22
C4	640	12.9	256	9.22	512	9.92	256	13.52
C5	256	14.84	896	9.98	640	13.42	256	9.12
DMSO	-	-	-	-	-	-	-	-
AMK	-	-	-	-	-	18.5	-	22.96
GEN	-	21.6	-	23.72	-	-	-	-

Antibacterial performance

Screening of all the study compounds was performed in terms of their antibacterial activities against varied types of bacterial strains through MIC by using the broth macro dilution procedure and inhibition zone via the disk diffusion method. The tests were repeated three times. MIC and inhibition zone values of all the compounds reported as the means of at least three determinations are depicted in Table 4. As seen in Table 4, all the compounds have nearly good inhibitory activities against all the bacterial strains compared to the positive controls (the standard drugs used for comparison purposes). Furthermore, all the compounds revealed stronger antibacterial activities in comparison to DMSO as a negative control. The antibacterial activities of the five complexes were found to be rather higher than those of thiourea ligand (L). Thus, the enhanced biological activity of this thiourea derivative (L) probably caused by the chelate formation was verified through the coordination with the transition metal ions. As a result, the polarities of the compounds and their lipophilic properties decreased and increased, respectively. The improved lipophilic features facilitated the interaction between these complexes and cell components and processes. Besides, the highest antibacterial activities of these complexes against all types of bacterial strains were witnessed. Bacterial growth inhibition was caused by all the compounds within a MIC range of 128-896 µg/mL. A kind of relationship between the antibacterial activities and LUMO energy and difference of LUMO and HOMO energies could be found through the precise examination of the theoretical results (Figure 2). In some cases, a linear relationship was further discovered between the mentioned features and the thickness of inhibition zones for the study standard bacterial strains. An example can be found in the linearity between the thickness of inhibition zones and differences of LUMO and HOMO energies in C2, C3, C4, and C5 compounds for P. aeruginosa.

This implies a higher antibacterial activity with a lower difference between LUMO and HOMO energies. $y=-1732.5x+257.67$, $R^2=0.9538$ is a linear equation for this relationship. Due to accessibility to suitable orbitals, a more proper interaction between the mentioned complexes and cell components and processes is implied by the relationships, some more instances of which have been exhibited in Figure 2

Conclusion

In this research study, the synthesis, characterization, theoretical calculation, and antibacterial properties of 5 first-row transition metal complexes containing a benzoyl thiourea derivative were investigated. Square-based pyramidal coordination could be concluded from the chemical structures

and configurations of the resulting complexes around the transition metal atoms. Some relationships between the antibacterial activities of these complexes and LUMO energy, as well as the difference between LUMO and HOMO energies, could be inferred from the theoretical calculations. The bacterial growth inhibition resulted from the functional abilities of all the synthesized compounds based on the antibacterial experiments. Following the discovery of antibacterial activities of these compounds, we are to investigate further the biological properties of other thiourea ligands participating in an interaction with transition metal complexes in the near future.

Acknowledgments

The authors are grateful to the University of Sistan and Baluchestan (USB) for supporting this study.

Orcid:

Javad Farzanfar: https://orcid.org/0000-0003-4816-2423

Ali Reza Rezvani: https://orcid.org/0000-0003-2681-9906

Hojat Samareh Delarami: https://orcid.org/0000-0001-6070-6943

References

[1] A.A. Isab, S. Nawaz, M. Saleem, M. Altaf, M. Monim-ul-Mehboob, S. Ahmad, H.S. Evans, *Polyhedron*, **2010**, *29*, 1251-1256.

[2] N. Dolan, D.P. Gavin, A. Eshwika, K. Kavanagh, J. McGinley, J.C. Stephens, *Bioorg. Med. Chem. Lett.*, **2016**, *26*, 630-635.

[3] P.R. Chetana, B.S. Srinatha, M.N. Somashekar, R.S. Policegoudra, *J. Mol. Struct.*, **2016**, *1106*, 352-365.

[4] P. Cui, X. Li, M. Zhu, B. Wang, J. Liu ,H. Chen, *Bioorg. Med. Chem. Lett.*, **2017**, *27*, 2234-2237.

[5] A. Bielenica, J. Stefańska, K. Stępień, A. Napiórkowska, E. Augustynowicz-Kopeć, G. Sanna, S. Madeddu, S. Boi, G. Giliberti, M. Wrzosek, *Eur. J. Med. Chem.*, **2015**, *101*, 111-125.

[6] I. Ullah, A. Shah, A. Badshah, N.A. Shah, R. Tabor, *Colloids Surf. A*, **2015**, *464*, 104-109.

[7] N.A. Mohamed, N.A.A. El-Ghany, M.M. Fahmy, *Int. J. Biol. Macromol.*, **2016**, *82*, 589-598.

[8] A.F. Elhusseiny, A. Eldissouky, A.M. Al-Hamza ,H.H.A.M. Hassan, *J. Mol. Struct.*, **2015**, *1100*, 530-545.

[9] S.S. Hassan, M.M. Shoukry, R.N. Shallan, R. van Eldik, *J. Coord. Chem.*, **2017**, *70*, 1761-1775.

[10] L. Qiao, J. Huang, W. Hu, Y. Zhang, J. Guo, W. Cao, K. Miao, B. Qin, J. Song, *J. Mol. Struct.*, **2017**, *1139*, 149-159.

[11] F. Bílek, T. Křížová, M. Lehocký, *Colloid. Surface. B.*, **2011**, *88*, 440-447.

[12] H.M. Faidallah, K.A. Khan, A.M. Asiri, *J. Fluorine. Chem.*, **2011**, *132*, 870-877.

[13] S. Karakuş, S. Rollas, *Farmaco* **2002**, *57*, 577-581.

[14] S.B. Tsogoeva, M.J. Hateley, D.A. Yalalov, K. Meindl, C. Weckbecker, K. Huthmacher, *Bioorg. Med. Chem.*, **2005**, *13*, 5680-5685.

[15] M. Mushtaque, F. Avecilla, M.S. Khan, Z.B. Hafeez, M.M.A. Rezvi, A. Srivastava, *J. Mol. Struct.*, **2017**, *1141*, 119-132.

[16] I.-J. Kang, L.-W. Wang, C.-C. Lee, Y.-C. Lee, Y.-S. Chao, T.-A. Hsu, J.-H. Chern, *Bioorg. Med. Chem. Lett.*, **2009**, *19*, 1950-1955.

[17] T. Yeşilkaynak, H. Muslu, C. Özpınar, F.M. Emen, R.E. Demirdöğen, N. Külcü, *J. Mol. Struct.*, **2017**, *1142*, 185-193.

[18] W. Hernández, E. Spodine, L. Beyer, U. Schröder, R. Richter, J. Ferreira, M. Pavani, *Bioinorg. Chem. Appl.*, **2005**, *3*, 299-316.

[19] E. Rodriguez-Fernandez, J.L. Manzano, J.J. Benito, R. Hermosa, E. Monte, J.J. Criado, *J. Inorg. Biochem.*, **2005**, *99*, 1558-1572.

[20] M.K. Rauf, A. Badshah, M. Gielen, M. Ebihara, D. de Vos, S. Ahmed, *J. Inorg. Biochem.*, **2009**, *103*, 1135-1144.

[21] H.-J. Zhang, X. Qin, K. Liu, D.-D. Zhu, X.-M. Wang, H.-L. Zhu, *Bioorg. Med. Chem.*, **2011**, *19*, 5708-5715.

[22] I.C. Mendes, M.A. Soares, R.G. dos Santos, C. Pinheiro, H. Beraldo, *Eur. J. Med. Chem.*, **2009**, *44*, 1870-1877.
[23] J. Farzanfar, K. Ghasemi, A.R. Rezvani, H.S. Delarami, A. Ebrahimi, H. Hosseinpoor, A. Eskandari, H.A. Rudbari, G. Bruno, *J. Inorg. Biochem.*, **2015**, *147*, 54-64.
[24] H. Arslan, N. Duran, G. Borekci, C. Koray Ozer, C. Akbay, *Molecules*, **2009**, *14*, 519-527.
[25] G. Li, D.-J. Che, Z.-F. Li, Y. Zhu ,D.-P. Zou, *New. J. Chem.*, **2002**, *26*, 1629-1633.
[26] C.K. Ozer, H. Arslan, D. Vanderveer, G. Binzet, *J. Coord. Chem.*, **2009**, *62*, 266-276.
[27] C. Lee, W. Yang, R.G. Parr, *Phys. Rev. B*, **1988**, *37*, 785.
[28] G. Micera, E. Garribba, *Int. J. Quantum Chem.*, **2012**, *112*, 2486-2498.
[29] G. Micera, V.L. Pecoraro, E. Garribba, *Inorg. Chem.*, **2009**, *48*, 5790-5796.
[30] S. Gorelsky, G. Micera, E. Garribba, *Chem. Eur. J.*, **2010**, *16*, 8167-8180.
[31] I. Wiegand, K. Hilpert, R.E.W. Hancock, *Nat. Protoc.*, **2008**, *3*, 163-175.
[32] U. El-Ayaan, *J. Mol. Struct.*, **2011**, *998*, 11-19.
[33] L. Sacconi, *Pure Appl. Chem.*, **1968**, *17*, 95-128.
[34] W.J. Geary, *Coord. Chem. Rev.*, **1971**, *7*, 81-122.
[35] W. Yang, H. Liu, M. Li, F. Wang, W. Zhou, J. Fan, *J. Inorg. Biochem.*, **2012**, *116*, 97-105.

How to cite this article: Javad Farzanfar, Elahe Abdolahe, Amir Eskandari, Ali Reza Rezvani*, Hojat Samareh Delarami. Synthesis, characterization, density functional theory (DFT) calculation and antibacterial activities of five-coordinate complexes of some first-row transition metals containing a benzoyl thiourea derivative. *Eurasian Chemical Communications*, 2020, 2(9), 961-971.
Link: http://www.echemcom.com/article_113346.html